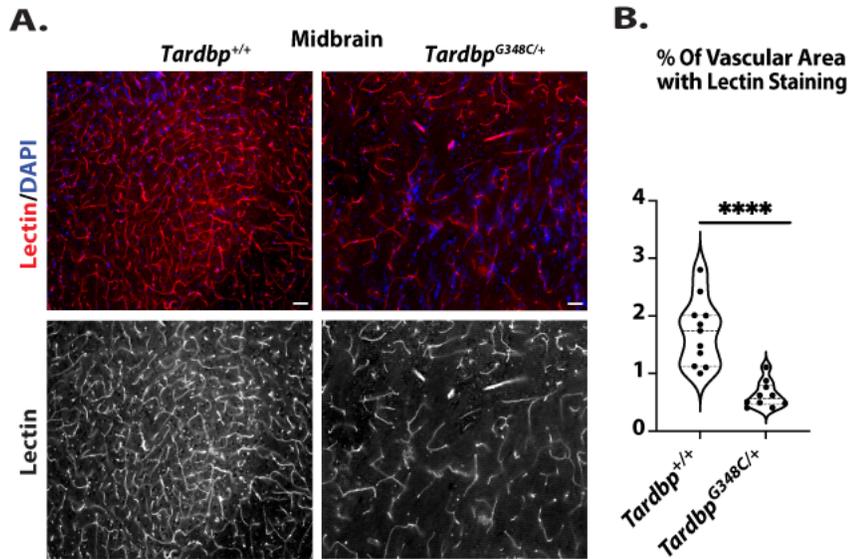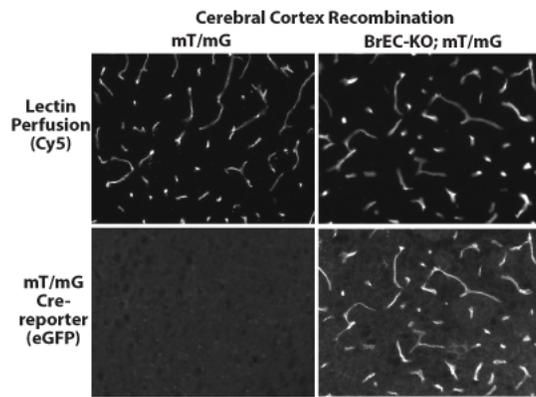**SI Figure 1. Assessment of Blood-Brain Barrier Permeability. (A)** The representative immunofluorescence images of 3kDa Texas Red-dextran leakage in mouse midbrain sections from 10-11-month-old mice (n=3 *Tardbp$^{+/+}$* and n=3 *Tardbp$^{G348C/+)}$* are shown. **(C)** NHS-Biotin. **(B, D)** Quantification of data, with each data point representing the fluorescence image intensity in one image. multiple images per mouse. Scale bars, 50 μm. Data are presented as means ± SEM. Statistical analysis was conducted using an unpaired Mann Whitney test, with significance levels indicated as follows: ***P 0.0001, ****P<0.0001.

SI Figure 2. Evaluation of Tomato-Lectin Perfusion. (A) The representative immunofluorescence images of Tomato-lectin perfusion in mouse midbrain sections from 10-11-month-old mice (n=3 *Tardbp*$^{+/+}$ and n=3 *Tardbp*$^{G348C/+)}$ are shown. (B) Quantification of data, with each data point representing the fluorescence image intensity in one image. Multiple images per mouse. Scale bars, 50 μm. Data are presented as means ± SEM. Statistical analysis was conducted using an unpaired Mann Whitney test, with significance levels indicated as follows: ****P<0.0001.
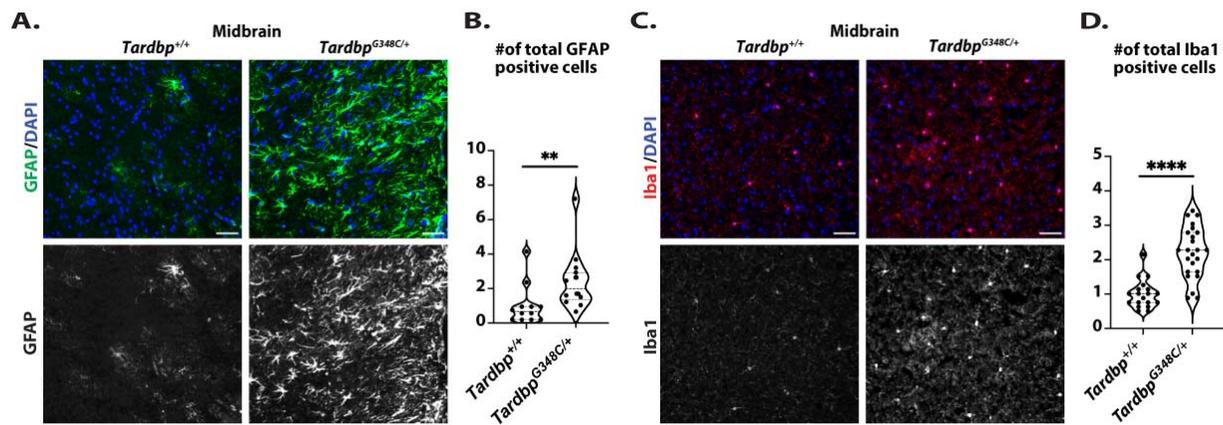
SI Figure 3. Assessment of Astrocyte (GFAP) and Microglia (Iba1) Activation. (A) The representative immunofluorescence images of GFAP staining of astrocytes, and (C) Iba1 staining of microglia in the mouse midbrain reveal consistent results across $Tardbp^{+/+}$ mice (n=3) and $Tardbp^{G348C/+}$ mice (n=3). (B, D) Quantification of data with each data point representing the number of activated cells in an image. multiple images per mouse. Scale bars, 50 μm. Data are presented as means ± SEM. Statistical analysis was conducted using an unpaired Mann Whitney test, with significance levels indicated as follows: **P 0.0023, ****P<0.0001.

SI Figure 4. Slco1c1-CreERT2 is active in cortical vasculature. (A) BrEC-KO mice with mT/mG Cre reporter were treated with Tamoxifen and collected with Dylight649 lectin perfusion 12 weeks later. eGFP indicates Cre activity in cortical vessels.
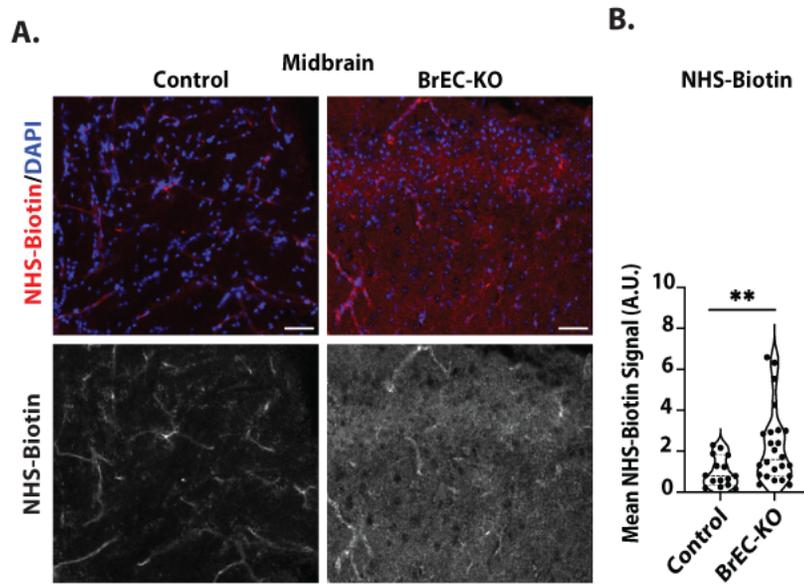
SI Figure 5. Blood brain barrier disruption in _Tardbp_ BrEC-KO, midbrain. (A) The representative immunofluorescence images of NHS-biotin leakage in mouse midbrain sections from 3-7-month-old mice (n=3 BrEC-KO and n=3 littermate controls) are shown. B) Quantification signal, with each data point representing the fluorescence image intensity from one image, multiple images per mouse. Scale bars, 50 μm . Data is presented as means ± SEM. Statistical analysis was performed using an unpaired two-tailed Mann Whitney test, with significance levels indicated as follows: **P⊡0.0096.
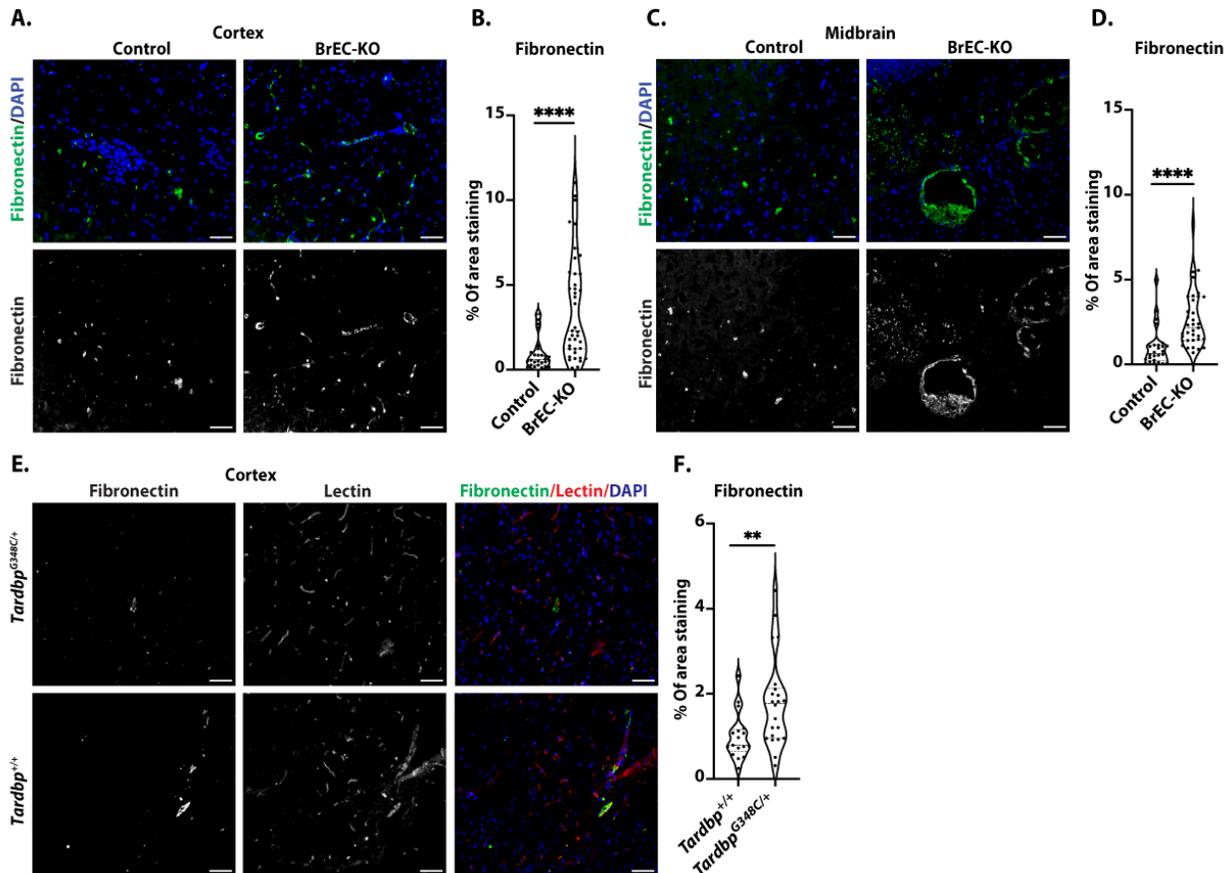
SI Figure 6. Increased Fibronectin Expression in *Tardbp* BrEC-KO and *Tardbp*$^{G348C/+}$ mice. (A) Representative immunofluorescence images of fibronectin in mouse cortex and (C) midbrain sections from 8-11-month-old mice (n=3 BrEC-KO and n=3 littermate controls) are presented. Additionally, (E) representative immunofluorescence images of fibronectin in mouse cortex sections from 10-11-month-old mice (n=3 *Tardbp*$^{+/+}$ and n=3 *Tardbp*$^{G348C/+)}$ are shown. (B, D, F) Quantification signal, with each data point representing the fluorescence image intensity from one image, multiple images per mouse. Scale bars, 50 µm. Data is presented as means ± SEM. Statistical analysis was performed using an unpaired two-tailed Mann Whitney test, with significance levels indicated as follows: **P⬚0.0044, ****P<0.0001.
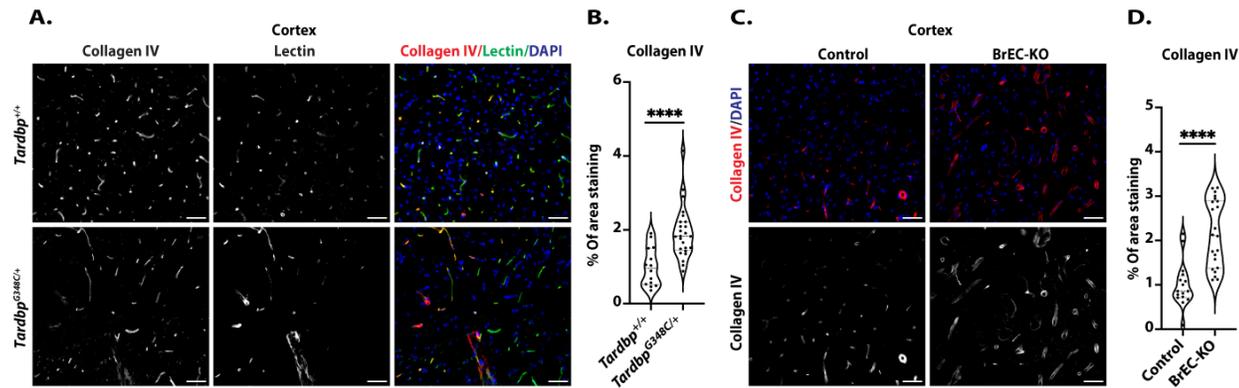
SI Figure 7. Increased Collagen IV Expression in *Tardbp* BrEC-KO and *Tardbp*^G348C/+ mice. (A) Representative immunofluorescence images of Collagen IV in mouse cortex sections from 10-11-month-old mice (n=3 *Tardbp*^+/+ and n=3 *Tardbp*^G348C/+) are presented. Additionally, (C) representative immunofluorescence images of Collagen IV in mouse cortex sections from 8-11-month-old mice (n=3 BrEC-KO and n=3 littermate controls) are shown. (B&D) Quantification signal, with each data point representing the fluorescence image intensity from one image, multiple images per mouse. Scale bars, 50 μm . Data is presented as means ± SEM. Statistical analysis was performed using an unpaired two-tailed Mann Whitney test, with significance levels indicated as follows: ****P<0.0001.
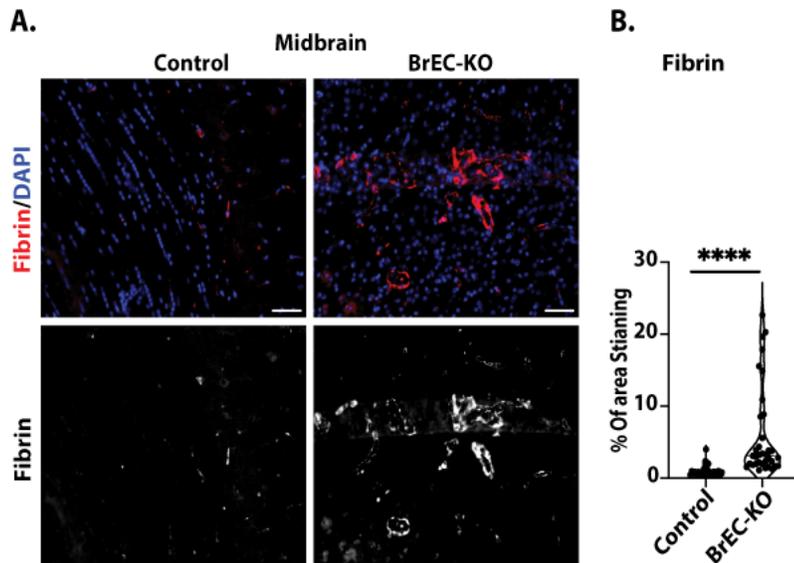
SI Figure 8. Fibrin Deposition in BrEC-KO Mouse Midbrain. (A) Representative immunofluorescence images of fibrin deposition in mouse midbrain sections from 8-11-month-old mice (n=3 BrEC-KO and n=3 littermate controls) are shown. (B) Quantification signal, with each data point representing the fluorescence image intensity from one image, multiple images per mouse. Scale bars, 50 µm. Data is presented as means ± SEM. Statistical analysis was performed using an unpaired two-tailed Mann Whitney test, with significance levels indicated as follows: ****P<0.0001.
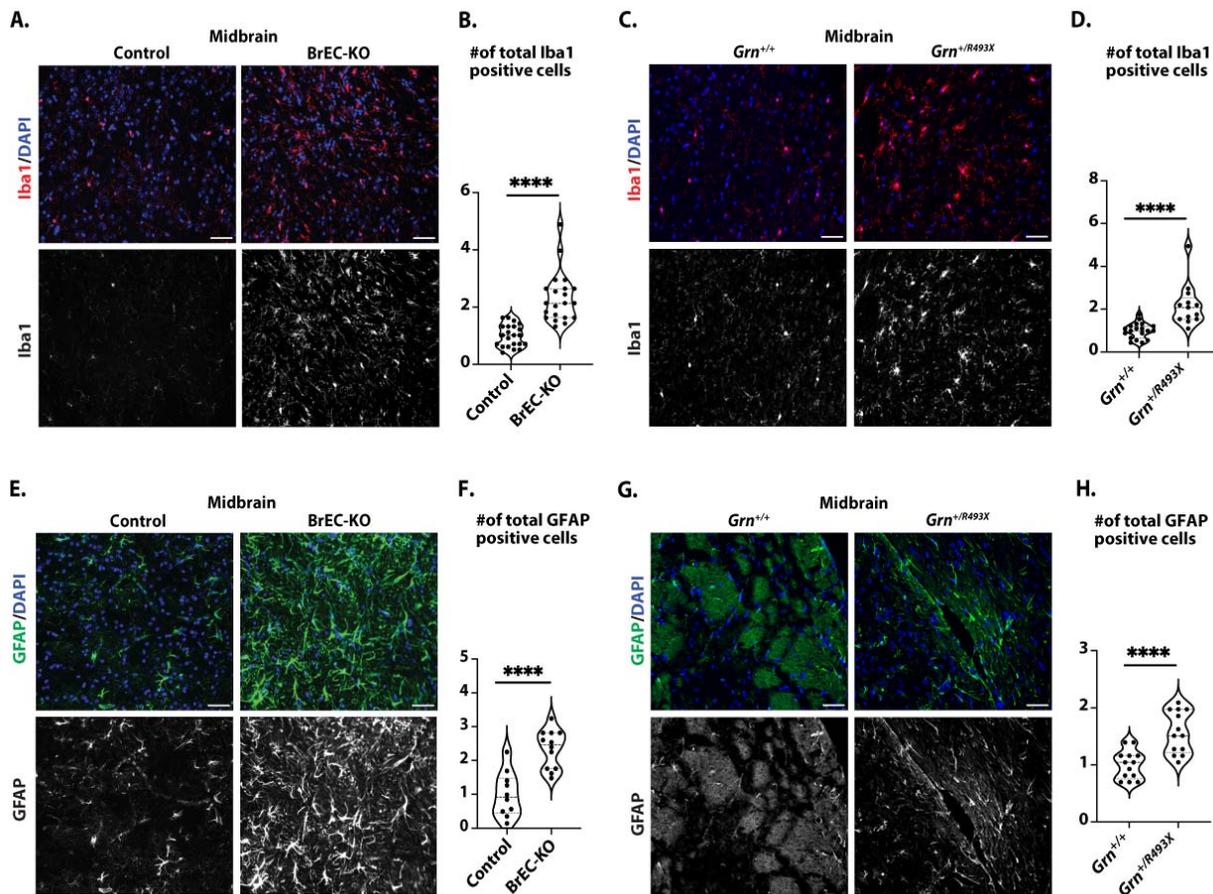
SI Figure 9. Assessment of Astrocyte (GFAP) and Microglia (Iba1) Activation. (A, C) Representative immunofluorescence images of Iba1 staining of microglia in the mouse midbrain reveal consistent results across (n=3 BrEC-KO and littermate controls mice (n=3), as well as n=3 $Grn^{R493X/+}$ and littermate controls mice (n=3) and (E, G) GFAP staining of astrocytes reveals a substantial increase in astrocyte numbers, resembling astrogliosis observed in FTD. (B, D, F, H) Quantification of data with each data point representing the number of activated cells in an image. multiple images per mouse. Scale bars, 50 μm. Data are presented as means ± SEM. Statistical analysis was conducted using an unpaired two-tailed Mann Whitney test, with significance levels indicated as follows: ****P<0.0001.
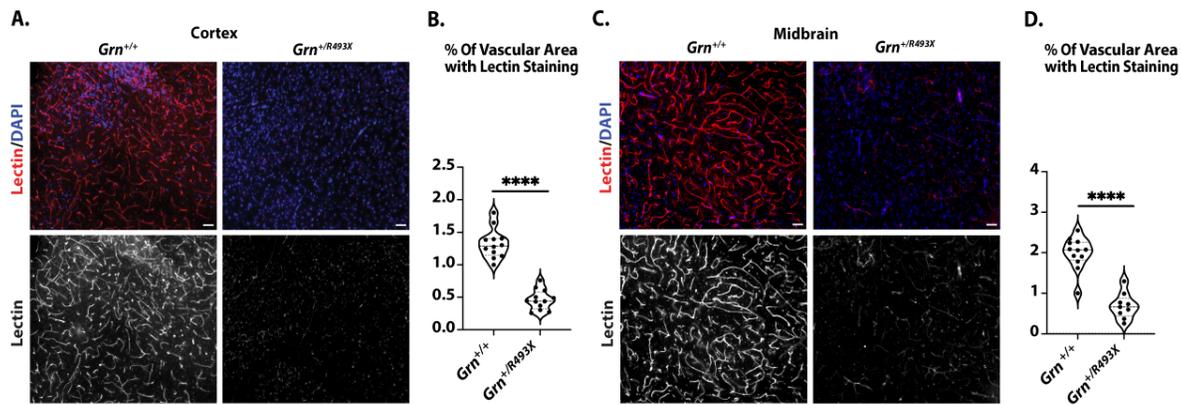
SI Figure 10. Evaluation of Tomato-Lectin Perfusion. (A) The representative immunofluorescence images of Tomato-lectin perfusion in mouse midbrain sections from 25–27-month old mice (n=3 $Grn^{R493X/+}$ and littermate control mice (n=3) are shown. (B) Quantification of data, with each data point representing the fluorescence image intensity in one image. Multiple images per mouse. Scale bars, 50 μm. Data are presented as means ± SEM. Statistical analysis was conducted using an unpaired Mann Whitney test, with significance levels indicated as follows: ****P<0.0001
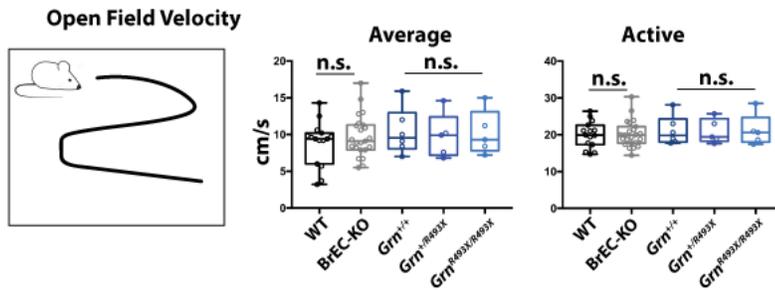
SI Figure 11. Behavioral Assessment of BrEC-KO Mice, Littermate Controls, and *Grn+*/R493X Knock-in Mouse Model of Frontotemporal Lobe Dementia (FTLD) in Open Field Velocity. BrEC-KO and littermate controls were assessed in behavioral core along with a knock-in mouse model of Frontal Temportal Lobe Dementia (FTLD, *Grn+*/R493X). No difference was observed in open field velocity.